

A numerical study on natural convection in an inclined square enclosure containing internal heat sources

H.-O. MAY

Technische Entwicklung, BASF AG, D-6700 Ludwigshafen, F.R.G.

(Received 12 January 1990)

Abstract—The two-dimensional conservation equations are solved numerically for natural convection in an inclined square box bounded by four rigid plates of constant temperature containing uniformly distributed internal energy sources. Two different numerical schemes are applied, the first is an ADI technique where vorticity and streamfunction are used, and the second is a hybrid method using primitive variables. Inclination angles from the horizontal of 0, 15, 30 and 45 deg and Rayleigh numbers from 10^4 to 1.5×10^7 are studied, the Prandtl number is 7 throughout. For $\theta = 0$ deg and $Ra \geq 5 \times 10^4$ an oscillating solution is achieved. The numerical results are compared in detail with an experimental study of Lee and Goldstein (*J. Heat Transfer* **110**, 345–349 (1988)).

INTRODUCTION

THE NATURAL convection in a confined enclosure has been examined extensively for the case when the flow was driven by a temperature gradient between the walls. Yang [1] and Ostrach [2] have presented surveys about experimental and numerical studies with a detailed list of references.

Thermal convection in a fluid with internal energy sources is very important in the theory of thermal ignition where heat sources within the fluid are driven by an exothermal chemical reaction. Here the thermal gradients originated by the chemical reaction can be the driving force for the onset of natural convection which markedly enhance the rate of heat transfer in comparison to a purely conductive mechanism. Numerical work on this problem has been presented by Merzhanov and Shtessel [3] and Jones [4], who studied a homogeneous zero-order reaction, whereas a first-order exothermal chemical reaction is described by Kopylov and Makhviladze [5]. Gray and Kostin [6] considered an adiabatic square enclosure in which a catalytic reaction occurs at the two side walls.

Emara and Kulacki [7] studied numerically the thermal convection in an enclosure which is driven by uniform heat sources. Their results are in good agreement with experimental data. Acharya and Goldstein [8] presented a numerical investigation of two-dimensional natural convection of air in an exothermally heated inclined box containing uniformly distributed internal heat sources.

The purpose of this paper is the numerical study of the flow in a confined enclosure being driven by uniform heat sources within and the examination of the temperature field and heat transfer to the walls. Experiments which are described by Lee and Goldstein [9] are simulated using two different

numerical schemes. The fluid used in these experiments was distilled water with NaCl added in order to raise the electrical conductivity. The thermophysical properties of the fluid were very close to those of pure water. A 60 Hz a.c. was passed from one silver-plated copper plate to the opposing one through the water to provide a relatively uniform internal heat source. The temperature distribution was measured using a Mach-Zehnder interferometer. A schematic drawing of the apparatus is shown in Fig. 1.

GOVERNING EQUATIONS

We start from the conservation equations of mass, momentum and energy for a Newtonian fluid the motion of which is laminar using the Boussinesq approximation. Three-dimensional effects are neglected here.

Using the dimensionless variables (see Fig. 1)

$$\begin{aligned}t &= \tau \frac{v}{L^2}, & x &= \frac{X}{L}, & y &= \frac{Y}{L} \\ u &= U \frac{L}{v}, & v &= V \frac{L}{v} \\ \vartheta &= \frac{8k}{HL^2}(T - T_0)\end{aligned}\quad (1)$$

the continuity, momentum and energy equation may be written as

$$\frac{\partial u}{\partial x} + \frac{\partial v}{\partial y} = 0 \quad (2)$$

$$\frac{\partial u}{\partial t} + u \frac{\partial u}{\partial x} + v \frac{\partial u}{\partial y} - \Delta u = - \frac{\partial p}{\partial x} + 8 \frac{R}{Pr} \vartheta \sin \Theta \quad (3)$$

NOMENCLATURE

g gravitational acceleration
 H energy source per unit time and volume
 k thermal conductivity
 Nu local Nusselt number, equation (18)
 \overline{Nu} average Nusselt number, equation (19)
 Nu^* modified Nusselt number, equation (20)
 n direction normal to the wall
 p dimensionless pressure
 Pr Prandtl number
 Ra Rayleigh number, equation (6)
 T temperature
 T_0 temperature at the wall
 t dimensionless time
 U, V velocity components in the X - and Y -directions
 u, v dimensionless velocity components
 X, Y Cartesian coordinates

x, y dimensionless coordinates.

Greek symbols

α thermal diffusivity of fluid
 β thermal expansion coefficient of fluid
 Θ inclined angle, Fig. 1
 ϑ dimensionless temperature
 ν kinematic viscosity of fluid
 τ time
 ψ streamfunction
 ω vorticity

Subscripts

B bottom wall
L left wall
R right wall
T top wall.

$$\frac{\partial v}{\partial t} + u \frac{\partial v}{\partial x} + v \frac{\partial v}{\partial y} - \Delta v = - \frac{\partial p}{\partial y} + 8 \frac{Ra}{Pr} \vartheta \cos \Theta \quad (4)$$

$$u = \frac{\partial \psi}{\partial y}, \quad v = - \frac{\partial \psi}{\partial x} \quad (10)$$

$$\frac{\partial \vartheta}{\partial t} + u \frac{\partial \vartheta}{\partial x} + v \frac{\partial \vartheta}{\partial y} - \frac{1}{Pr} \Delta \vartheta = \frac{8}{Pr} \quad (5)$$

so that the continuity equation (2) is identically satisfied. The vorticity ω is defined by

$$\omega = \frac{\partial v}{\partial x} - \frac{\partial u}{\partial y} \quad (11)$$

The dimensionless parameters characterizing the system are the inclination angle θ , the Rayleigh number

$$Ra = \frac{g\beta}{\alpha\nu} \left(\frac{L}{2} \right)^3 \frac{Hl^2}{8k} \quad (6)$$

and from equations (10) and (11) follows the relation between ψ and ω by a Poisson equation

$$\Delta \psi = -\omega. \quad (12)$$

and the Prandtl number

$$Pr = \frac{\nu}{\alpha} \quad (7)$$

In terms of ψ and ω the momentum equations (3) and (4) yield

which was chosen to be constant here.

$$\frac{\partial \omega}{\partial t} + \frac{\partial \psi}{\partial y} \frac{\partial \omega}{\partial x} - \frac{\partial \psi}{\partial x} \frac{\partial \omega}{\partial y} - \Delta \omega$$

The boundary conditions are

$$u = v = \vartheta = 0 \quad \text{for } x = 0, 1 \quad \text{and } y = 0, 1 \quad (8)$$

$$= 8 \frac{Ra}{Pr} \left(\frac{\partial \vartheta}{\partial x} \cos \Theta - \frac{\partial \vartheta}{\partial y} \sin \Theta \right) \quad (13)$$

and the initial conditions become

$$u = v = \vartheta = 0 \quad \text{at } t = 0. \quad (9)$$

and the energy equation (5) may be written as

Now we introduce the streamfunction ψ satisfying

$$\frac{\partial \vartheta}{\partial t} + \frac{\partial \psi}{\partial y} \frac{\partial \vartheta}{\partial x} - \frac{\partial \psi}{\partial x} \frac{\partial \vartheta}{\partial y} - \frac{1}{Pr} \Delta \vartheta = \frac{8}{Pr} \quad (14)$$

The boundary conditions become

$$\psi = 0, \quad \frac{\partial \psi}{\partial n} = 0, \quad \vartheta = 0$$

$$\text{for } x = 0, 1 \quad \text{and } y = 0, 1 \quad (15)$$

where n is the direction normal to the wall. The boundary condition for ω will be discussed later. The initial conditions are

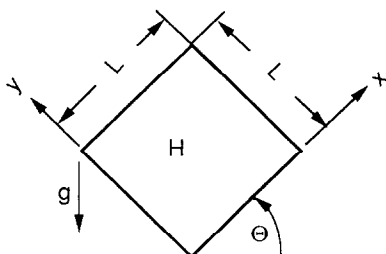


FIG. 1. Schematic diagram of the enclosure.

$$\psi = \omega = \vartheta = 0 \quad \text{for all } x, y. \quad (16)$$

SOLUTION PROCEDURE

The two-dimensional alternating-direction-implicit (ADI) method is used (compare Brian [10] and Borthwick [11]) for the solution of the vorticity and energy equation. The streamfunction equation is solved by the successive-over-relaxation (SOR) procedure.

The first and second derivatives in space are approximated by central differences. Each time-step is divided into two halves. For the first half time-step t_n to $t_{n+1/2}$ derivatives with respect to one space direction are represented by finite-difference analogues evaluated at $t_{n+1/2}$ whereas those with respect to the other direction are evaluated at t_n and are already known. In the next half time-step from $t_{n+1/2}$ to t_{n+1} the reverse procedure is used. Backward differences are used for approximating the time derivatives.

The boundary condition for the vorticity is calculated by a three-point forward or backward scheme for the streamfunction (see Roache [12]). This relation yields

$$\pm \frac{1}{2}\omega_m = \psi_{m\pm 1}/(\Delta n)^2 \tag{17}$$

where Δn is the mesh size and where the sign depends on the fact if n is the negative or positive x - or y -direction.

Moreover, a second numerical scheme was used in order to compare the results. Here we used a staggered grid procedure in primitive variables with a hybrid differencing scheme and a fully implicit scheme for evaluating the time-derivatives as described by Patankar [13] and Markatos and Pericleous [14].

GRID DEPENDENCY

As described later it was not possible to receive a stable steady solution for $\theta = 0$ deg and for a Rayleigh number of 5×10^4 or greater (the Prandtl number was 7 throughout). Several grid sizes and time steps are used in order to examine the grid dependency. The results for the case $Ra = 10^5$, $\theta = 0$ and 15 deg are given in Table 1. Three grids are considered here. The time of oscillation T_{oscill} the maximum and minimum temperatures at $x = y = 1/2$ for the case $\theta = 0$ deg and the maximum temperature in the field for the case $\theta = 15$ deg are given. Because of the minor differences for the 41×41 and 61×61 grids and because of the consumption of computer time the 41×41 grid is used for further calculations.

Table 1. Grid dependency for unsteady and steady solution ; $Ra = 10^5$

| $NX \times NY$ | T_{oscill} | $\Theta = 0$ deg | $\Theta = 15$ deg |
|----------------|--------------|---|-------------------|
| | | $\vartheta_{min}-\vartheta_{max}$ ($x = 0.5, y = 0.5$) | ϑ_{max} |
| 21 x 21 | 0.318 | 0.170-0.192 | 0.259 |
| 41 x 41 | 0.363 | 0.181-0.202 | 0.264 |
| 61 x 61 | 0.376 | 0.183-0.204 | 0.265 |

RESULTS AND DISCUSSION

The parameters for the numerical treatment are chosen in such a way that a comparison with the experimental results of Lee and Kulacki is possible. The Prandtl number is 7 and the Rayleigh numbers are 10^4 , 5×10^4 , 10^5 and 1.5×10^5 . For each Rayleigh number the inclined angles are selected as 0, 15, 30 and 45 deg.

Twelve sets of isotherms and flow patterns are shown in Figs. 2 and 3. The position of the maximum temperature is higher than for pure conduction and the influence of natural convection can be observed for all Rayleigh numbers. There is a strong pair of counter-rotating rolls for the inclined enclosure as can be seen from Fig. 3. The hot interior fluid moves upward in the middle along the line nearly parallel to the direction of gravity, then turns to the direction of the upper edge and divides the whole cross-section into two halves. The flow divides at the top and moves downward separately along the cold side walls.

In Table 2(a) the values of maximum temperature are given as they were observed by Lee and Kulacki. In Table 2(c) the computed values as evaluated with the ADI method and in Table 2(b) the values as computed using the hybrid method with primitive variables are given. The peak fluid temperature becomes lower at higher Rayleigh numbers because of the stronger convective motion, and the peak temperature is essentially independent of the inclined angle, if $\theta \geq 15$ deg.

The positions of the maximum temperature for $\theta = 30$ and 45 deg are given in Table 3. The position moves continuously toward the upper top case as the Rayleigh number increases and reaches $x/L = 0.875$ and $y/L = 0.875$ at $Ra = 1.5 \times 10^5$.

All these observations and the description of heat transfer given later are in excellent agreement with experimental results for an inclined angle $\theta \geq 15$ deg.

For the horizontal case it is first assumed that the enclosure would be divided by a symmetry line in the middle and only half of the enclosure is calculated (0 deg sym in Table 2). The corresponding streamline patterns and isotherms are shown in Fig. 4. Obviously there exist two pairs of counter-rotating rolls for the horizontal enclosure and for $Ra \geq 5 \times 10^4$, as indicated in the paper of Lee and Kulacki, but the values of maximum temperature are too low for the case $Ra \geq 5 \times 10^4$. The discussion for this case will be continued in the next section.

HEAT TRANSFER

The local and average Nusselt numbers are defined in the same way as in the paper of Lee and Kulacki by

$$Nu = \frac{1}{2} \left| \frac{\partial \vartheta}{\partial n} \right|_{wall} \tag{18}$$

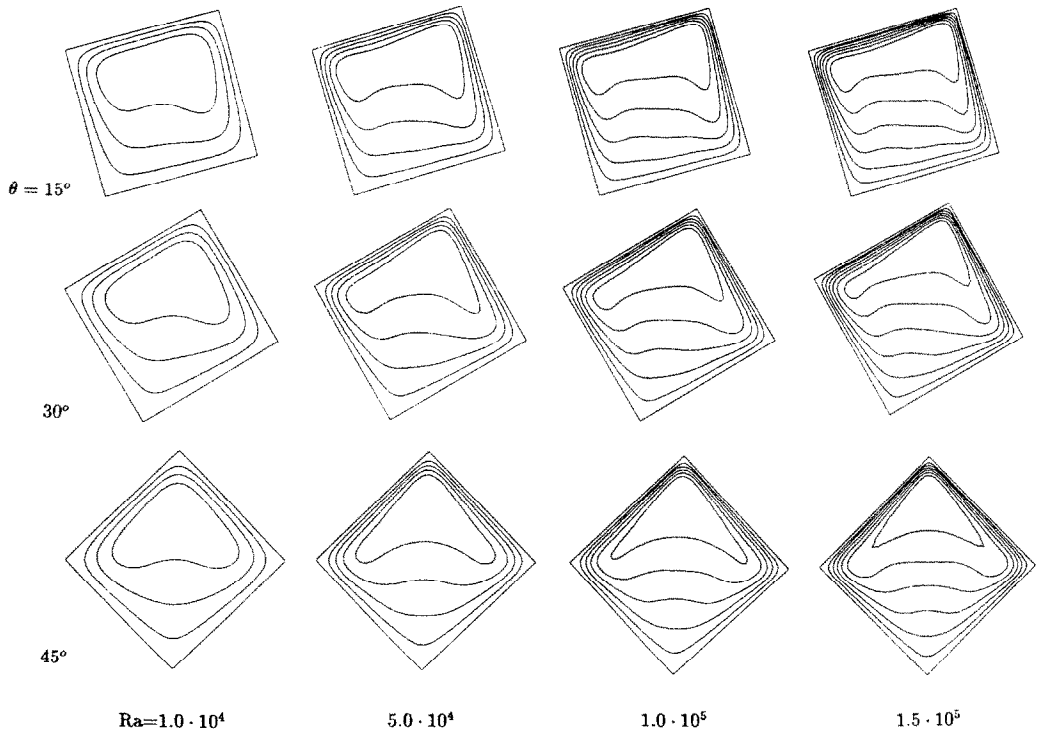


FIG. 2. Numerical isotherms.

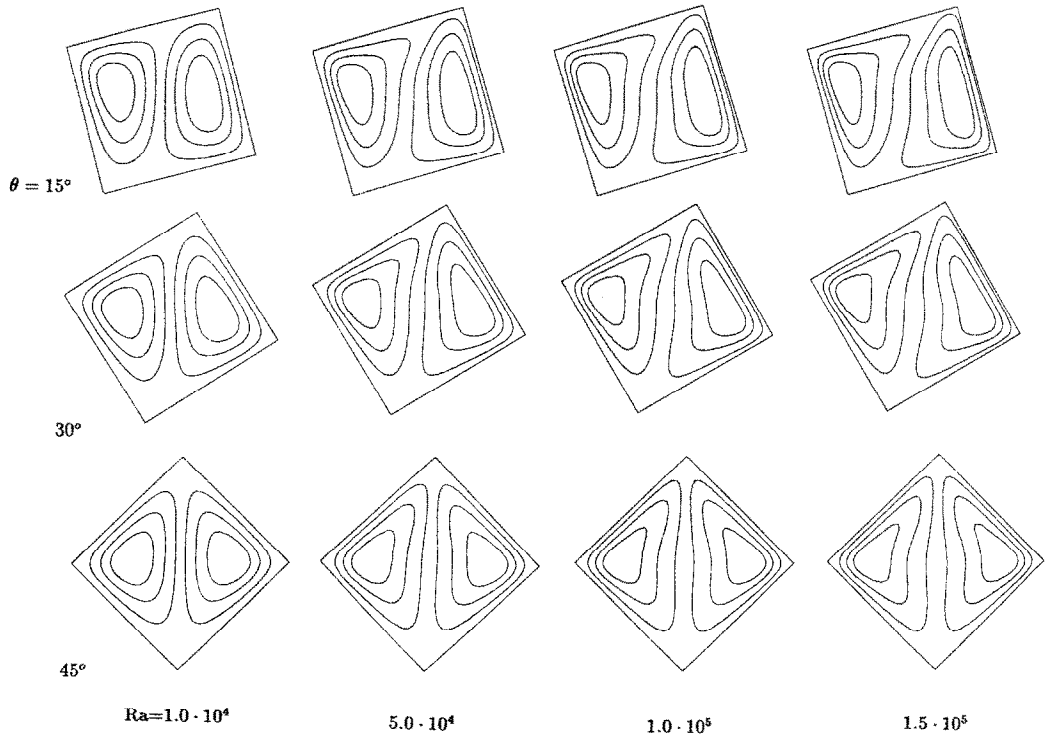


FIG. 3. Flow patterns.

Table 2. Comparison of numerical and experimental maximum temperatures

| (a) experimental | | | | | |
|-----------------------|---------|-------------|-------|-------|-------|
| Ra | Θ (deg) | | | | |
| | 0 | 15 | 30 | 45 | |
| 1 × 10 ⁴ | 0.387 | 0.388 | 0.389 | 0.389 | |
| 5 × 10 ⁴ | 0.293 | 0.294 | 0.293 | 0.293 | |
| 1 × 10 ⁵ | 0.253 | 0.258 | 0.257 | 0.257 | |
| 1.5 × 10 ⁵ | 0.236 | 0.238 | 0.233 | 0.234 | |
| (b) hybrid | | | | | |
| Ra | Θ (deg) | | | | |
| | 0 sym | 15 | 30 | 45 | |
| 1 × 10 ⁴ | 0.386 | 0.387 | 0.390 | 0.391 | |
| 5 × 10 ⁴ | 0.272 | 0.299 | 0.298 | 0.296 | |
| 1 × 10 ⁵ | 0.237 | 0.266 | 0.264 | 0.263 | |
| 1.5 × 10 ⁵ | 0.220 | 0.247 | 0.245 | 0.243 | |
| (c) ADI | | | | | |
| Ra | 0 sym | Θ (deg) | | | |
| | | 0 | 15 | 30 | 45 |
| 1 × 10 ⁴ | 0.382 | 0.382 | 0.387 | 0.390 | 0.392 |
| 5 × 10 ⁴ | 0.270 | 0.276–0.293 | 0.298 | 0.297 | 0.297 |
| 1 × 10 ⁵ | 0.235 | 0.241–0.256 | 0.264 | 0.262 | 0.261 |
| 1.5 × 10 ⁵ | 0.217 | 0.222–0.239 | 0.244 | 0.243 | 0.242 |

Table 3. Location of maximum temperature

| Ra | Θ = 30, 45 deg |
|-----------------------|----------------|
| | x, y |
| 1 × 10 ⁴ | 0.750, 0.750 |
| 5 × 10 ⁴ | 0.825, 0.825 |
| 1 × 10 ⁵ | 0.850, 0.850 |
| 1.5 × 10 ⁵ | 0.875, 0.875 |

$$\overline{Nu} = \int_0^1 Nu \, dn \tag{19}$$

where *n* denotes the *x*- or *y*-direction. We distinguish between left (index L), right (index R), bottom (index B), and top (index T) wall, respectively. In Fig. 5 several plots of the local Nusselt number distribution along each wall are given for the case *Ra* = 10⁵, θ = 15 deg and are compared with the conduction-only mode.

The influence of natural convection is investigated by a comparison of the local heat transfer rate with convection and conduction. For that, a modified local Nusselt number *Nu*⁺ as

$$Nu^+ = \frac{q_{conv}}{q_{2D,cond}} = Nu \left[\frac{16}{\pi^2} \sum_{n=0}^{\infty} \frac{1}{(2n+1)^2} \sin(2n+1)\pi x \tanh(2n+1) \frac{\pi}{2} \right] \tag{20}$$

is defined by Lee and Kulacki. Several *Nu*⁺ dis-

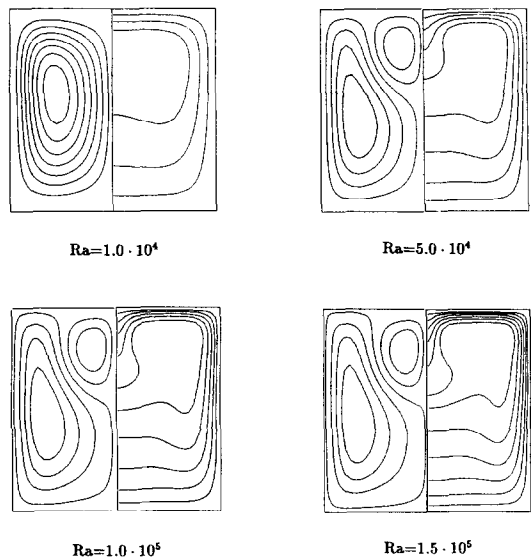


FIG. 4. Flow patterns and isotherms for horizontal enclosure ; symmetrical solution.

tributions are given for *Ra* = 1.5 × 10⁵ in Figs. 6 and 7. In Fig. 8 the variation of *Nu*_L⁺ at θ = 45 deg with Rayleigh number is shown.

Finally the variation of *Nu* with inclined angle and Rayleigh number is given in Fig. 9 (*Nu* = 1 corresponds to the two-dimensional conduction-only mode). Because of the reasons discussed before, only the cases θ > 15 deg are given. All the observations

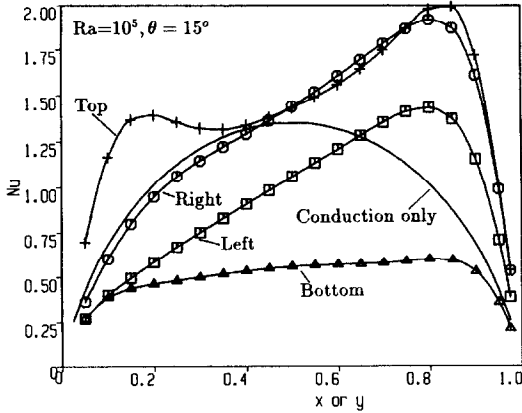


FIG. 5. Nusselt number distribution on each wall; $Ra = 10^3$, $\Theta = 15$ deg.

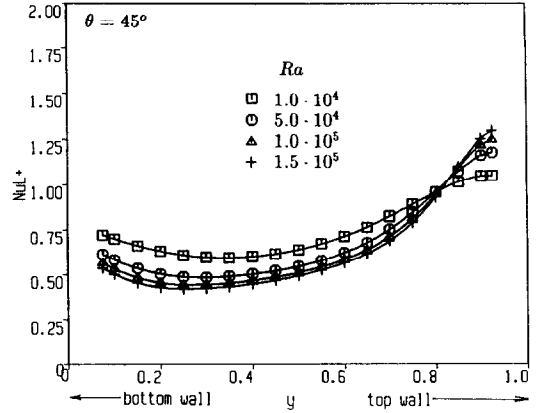


FIG. 8. Nu_t distribution at $\Theta = 45$ deg.

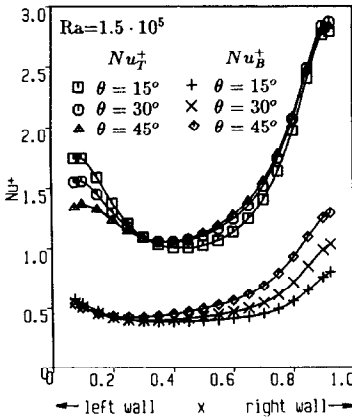


FIG. 6. Nu^+ distribution on the top and bottom walls; $Ra = 1.5 \times 10^5$.

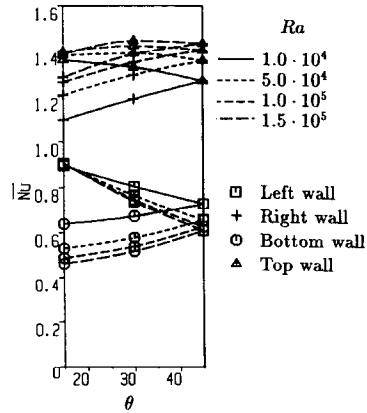


FIG. 9. Effect of inclined angle on Nu .

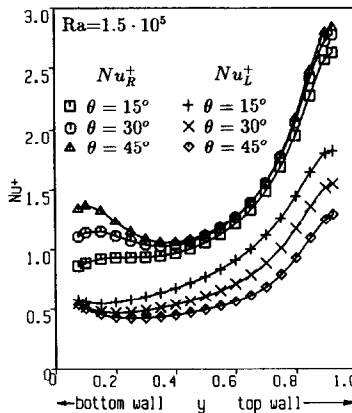


FIG. 7. Nu^+ distribution on the left and right walls; $Ra = 1.5 \times 10^5$.

and discussion made in the paper of Lee and Kulacki are also valid for the numerical simulation. But there seems to be one discrepancy in Fig. 9 of this paper being not consistent with the description which states

that "as the Rayleigh number increases Nu increases, with $Nu > 1$, on the top and right walls, and decreases with $Nu < 1$, on the bottom and left walls", Fig. 9 of Lee and Kulacki indicates for $\theta = 0$:

$$\overline{Nu}_T(1.5 \times 10^5) \leq \overline{Nu}_T(5 \times 10^4) \leq \overline{Nu}_T(1 \times 10^5) \leq \overline{Nu}_T(1 \times 10^4). \quad (21)$$

Probably the explanation for this non-monotone behaviour is the oscillating nature of the flow for the case $\theta = 0$ deg which results in an oscillation of \overline{Nu}_T as shown in Fig. 10 for the case $Ra = 5 \times 10^4$ and 10^5 .

In Fig. 10 the variation of \overline{Nu}_T for $\theta = 0$ deg, $Ra = 5 \times 10^4$ and 10^5 is shown and obviously the solution is oscillating for these cases. The results of the maximum temperature for the simulation without symmetry assumption are given in Table 2(c). The maximum temperature is oscillating between a lower and upper value and the measured value is between these numbers. For the cases $Ra = 1.5 \times 10^5$ and $\theta = 15, 30$ deg only slight oscillations could be observed.

Unfortunately it was not possible to receive a satisfactory result for the oscillating case when using the hybrid scheme. The solution was unsteady too, but

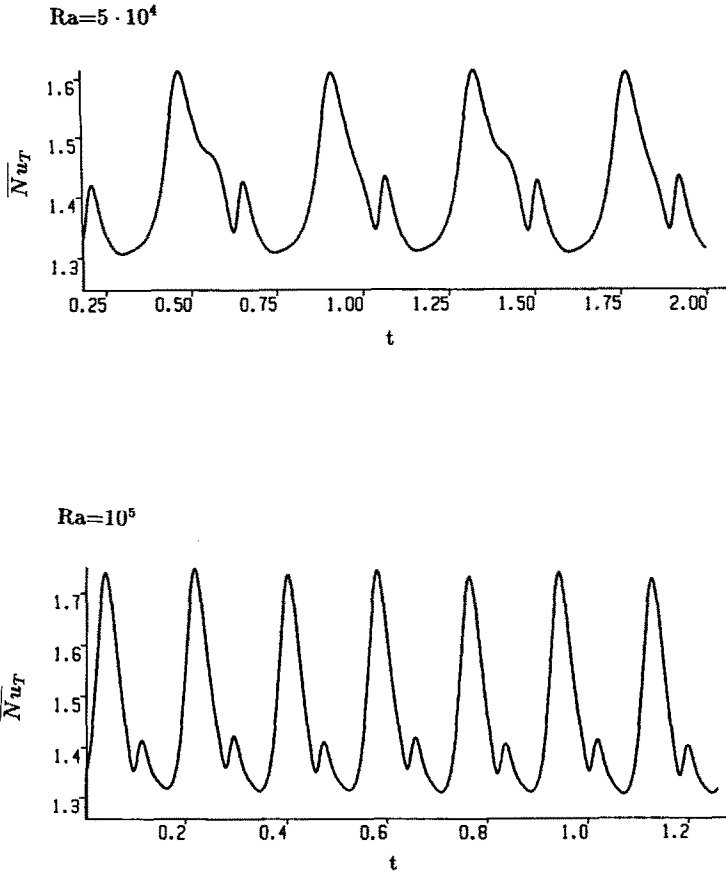


FIG. 10. \overline{Nu}_T as a function of time for $Ra = 5 \times 10^4$ and 10^5 .

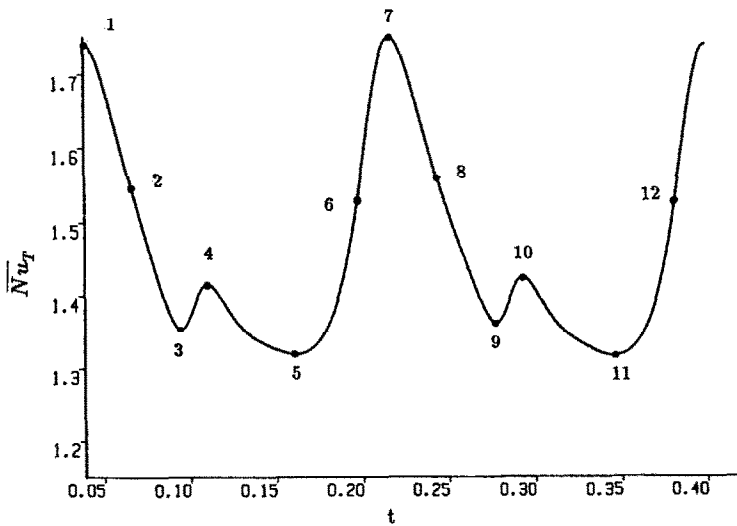


FIG. 11. \overline{Nu}_T as a function of time for $Ra = 10^5$ and one period of oscillation.

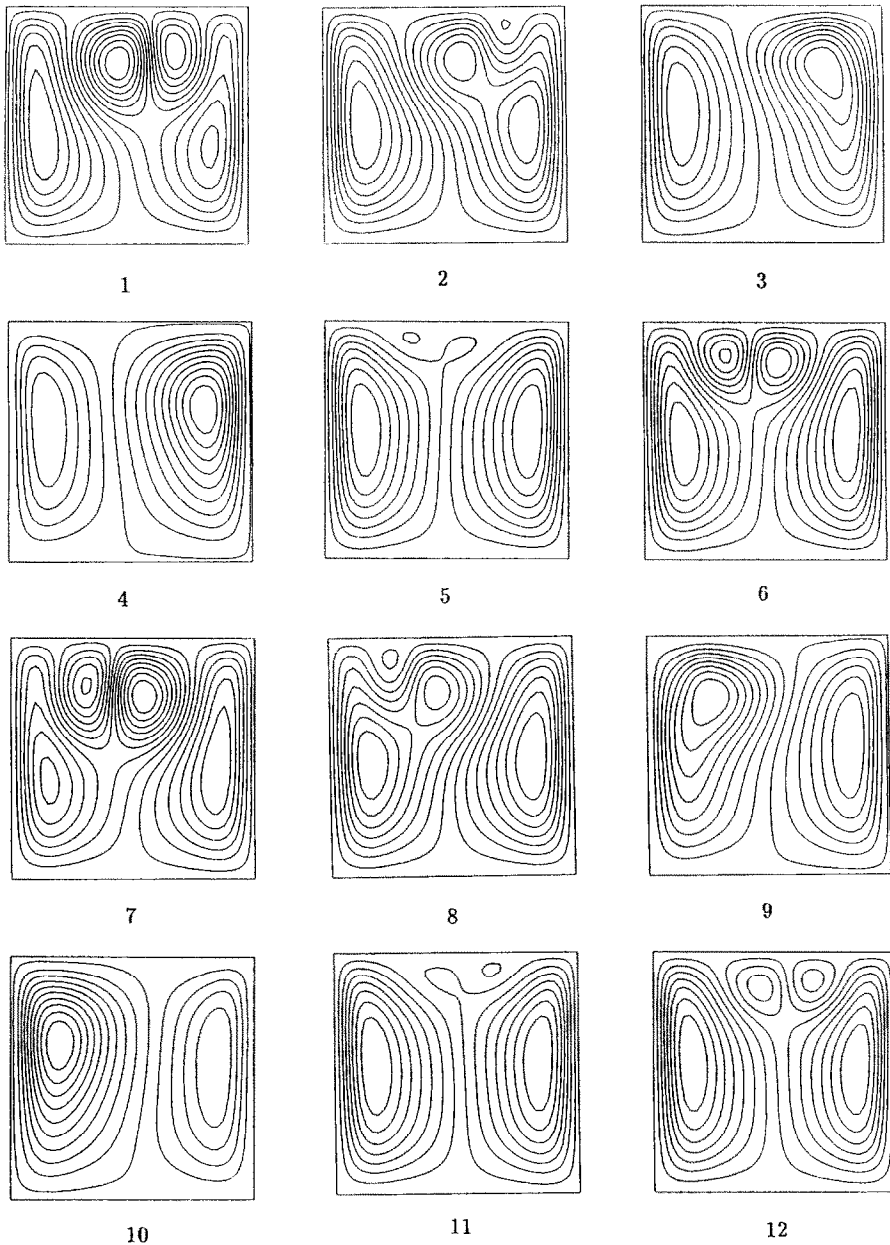


FIG. 12. Flow patterns during one period of oscillation.

even for very fine grids the result was strongly grid dependent and no limit could be observed. Probably this is a direct consequence of the excessive numerical damping due to the numerical viscosity being imposed by the upwind scheme (see Borthwick [11]).

Finally, Fig. 11 charts the variation of Nu_T with time for the case $\theta = 0$ deg and $Ra = 10^5$ for one cycle of oscillation. The corresponding streamline patterns are shown in Fig. 12. In the beginning at $t = t_1$ a pair of strong counter-rotating rolls is situated near the upper-centre portion of the enclosure. Then the left upper roll joins with the right main roll and the right

upper roll is destroyed (t_2, t_3, t_4). At $t = t_5$ two new upper rolls appear and enlarge, and from $t = t_7$ the whole procedure repeats itself being reflected at the symmetry line until the starting point t_1 is reached again.

CONCLUSION

The two-dimensional natural convection in an inclined square enclosure containing internal heat sources has been investigated numerically. Two different schemes have been applied, the first one was

an ADI procedure using vorticity and streamfunction and the second was a hybrid method using primitive variables. The temperature distribution and the heat transfer rates are compared with the experimental results of Lee and Goldstein, where interferograms were obtained using water of very low salinity for a square enclosure of 38.1 mm × 38.1 mm. The Prandtl number assumed was 7 and the Rayleigh number varied from 10^4 to 1.5×10^5 .

All the observations described by Lee and Kulacki are valid for the numerical simulation too. The results are in excellent agreement for an inclined angle of $\theta \geq 15$ deg. For $\theta = 0$ deg and $Ra \geq 5 \times 10^4$ a two-dimensional steady solution was only achieved when assuming symmetry conditions in the middle of the enclosure. When simulating the whole enclosure without the symmetry assumption an oscillating solution was achieved for $\theta = 0$ deg and $Ra \geq 5 \times 10^4$, indicating that the sets of counter-rotating rolls are unstable. These rolls appear and disappear during one cycle of oscillation.

In this work only the two-dimensional flow was considered. For future work it will be interesting to examine the whole three-dimensional flow in an inclined square enclosure containing heat sources.

REFERENCES

1. K. T. Yang, Transitions and bifurcations in laminar buoyant flows in confined enclosures, *J. Heat Transfer* **110**, 1191–1204 (1988).
2. S. Ostrach, Natural convection in enclosures, *J. Heat Transfer* **110**, 1175–1190 (1988).
3. A. G. Merzhanov and E. A. Shtessel, Free convection and thermal explosion in reactive systems, *Astronaut. Acta* **18**, 191–199 (1973).
4. D. R. Jones, Convective effects in enclosed, exothermically reacting gases, *Int. J. Heat Mass Transfer* **17**, 11–21 (1974).
5. G. G. Kopylov and G. M. Makhviladze, Influence of natural convection on the concentrational limits of ignition of a fuel mixture in a closed vessel, *Combust. Explosion Shock Waves* **19**, 135–141 (1983).
6. W. G. Gray and M. D. Kostin, Natural convection, diffusion and chemical reaction in a catalytic reactor: numerical results, *Chem. Engng J.* **8**, 1–10 (1974).
7. A. A. Emara and F. A. Kulacki, A numerical investigation of thermal connection in a heat-generating fluid layer, ASME Paper No. 79-HT-103 (1979).
8. S. Acharya and R. J. Goldstein, Natural convection in an externally heated vertical or inclined square box containing internal energy sources, *J. Heat Transfer* **107**, 855–866 (1985).
9. J.-H. Lee and R. J. Goldstein, An experimental study on natural convection heat transfer in an inclined square enclosure containing internal energy sources, *J. Heat Transfer* **110**, 345–349 (1988).
10. P. L. T. Brian, A finite-difference method of high-order accuracy for the solution of three-dimensional transient heat conduction problems, *A.I.Ch.E. J.* **7**, 367–370 (1961).
11. A. Borthwick, Comparison between two finite-difference schemes for computing the flow around a cylinder, *Int. J. Numer. Meth. Fluids* **6**, 275–290 (1986).
12. P. J. Roache, *Computational Fluid Dynamics*. Hermosa, Albuquerque, New Mexico (1985).
13. S. V. Patankar, *Numerical Heat Transfer and Fluid Flow*. Hemisphere, Washington, DC (1980).
14. N. C. Markatos and K. A. Pericleous, Laminar and turbulent natural convection in an enclosed cavity, *Int. J. Heat Mass Transfer* **27**, 755–772 (1984).

ETUDE NUMERIQUE DE LA CONVECTION NATURELLE DANS UNE CAVITE CARREE INCLINEE CONTENANT DES SOURCES THERMIQUES INTERNES

Résumé—Les équations bidimensionnelles de conservation sont résolues numériquement pour la convection naturelle dans une boîte carrée inclinée, limitée par quatre parois rigides à température constante et qui contient des sources thermiques internes uniformément distribuées. On applique deux schémas numériques différents; le premier est la technique ADI avec fonction de courant et vorticit  et l'autre est une m thode hybride utilisant les variables primaires. On consid re des angles d'inclinaison,   partir de l'horizontale de 0, 15, 30 et 45 degr s, des nombres de Rayleigh entre 10^4 et $1,5 \times 10^5$ et un nombre de Prandtl  gal   7. Pour $\theta = 0$ et $Ra \geq 5 \times 10^4$ on obtient une solution oscillante. Les r sultats num riques sont compar s en d tail avec l' tude exp rimentale de Lee et Goldstein (*J. Heat Transfer* **110**, 345–349 (1988)).

NUMERISCHE UNTERSUCHUNG DER NAT RLICHEN KONVEKTION IN EINEM ANGESTELLTEN QUADRATISCHEN BEH LTER MIT INNEREN W RMEQUELLEN

Zusammenfassung—F r die nat rliche Konvektion in einem angestellten quadratischen Beh lter wurden die zweidimensionalen Erhaltungsgleichungen numerisch gel st. Der Beh lter war durch vier starre W nde, die auf konstanter Temperatur gehalten wurden, begrenzt und enthielt r umlich und zeitlich konstante W rmequellen. Es wurden zwei verschiedene numerische Verfahren verwendet: Das erste war ein ADI-Verfahren, bei dem Stromfunktion und Wirbelst rke benutzt wurden, das zweite war ein Hybridverfahren, wo Druck und Geschwindigkeiten verwendet wurden. Die Anstellwinkel von der Horizontalen waren 0, 15, 30 und 45 Grad, und die Rayleigh-Zahlen variierten von 10^4 bis $1,5 \times 10^5$, die Prandtl-Zahl war immer 7. F r $\theta = 0$ und $Ra \geq 5 \times 10^4$ ergaben sich oszillierende L sungen. Die numerischen Ergebnisse wurden im einzelnen mit einer experimentellen Untersuchung von Lee und Goldstein (1988) verglichen.

ЧИСЛЕННОЕ ИССЛЕДОВАНИЕ ЕСТЕСТВЕННОЙ КОНВЕКЦИИ В НАКЛОННОЙ ПОЛОСТИ КВАДРАТНОГО СЕЧЕНИЯ, СОДЕРЖАЩЕЙ ВНУТРЕННИЕ ИСТОЧНИКИ ТЕПЛА

Аннотация—Численно решены двумерные уравнения сохранения для естественной конвекции в наклонной полости квадратного сечения. Полость ограничена четырьмя жесткими пластинами, на которых задана постоянная температура, и содержит однородно распределенные внутренние источники энергии. Использовались две различные численные схемы: неявный метод переменных направлений, в котором вводятся завихренность и функция тока, и смешанный метод, построенный на основе первичных переменных. Исследуемые углы наклона к горизонтали составляли 0° , 15° , 30° и 45° , число Рэлея изменялось в диапазоне от 10^4 до $1,5 \times 10^5$, а число Прандтля во всех случаях равнялось 7. При $\theta = 0^\circ$ и $Ra \geq 5 \times 10^4$ получено осциллирующее решение. Проведено тщательное сравнение полученных численных результатов с результатами экспериментального исследования Ли и Голдстейна (*J. Heat Transfer* **110**, 345–349 (1988)).